AIMS Energy, 9(5): 915–933.
DOI: 10.3934/energy.2021043
Received: 01 May 2021
Accepted: 12 July 2021
Published: 21 July 2021

http://www.aimspress.com/journal/energy

Research article

An Electro-Thermal Model based fast optimal charging strategy for Li-ion batteries

Saad Jarid and Manohar Das*

Department of Electrical and Computer Engineering, Oakland University, Rochester, MI 48309, USA

* **Correspondence:** Email: das@oakland.edu; Tel: +2483702237.

Abstract: This paper utilizes an integrated electro-thermal model of a lithium-ion battery to search for an optimal multistage constant current charge pattern that will minimize the total charging time of the battery, while restricting its temperature rise in each stage within safe limits. The model consists of two interlinked components, an electrical equivalent circuit model to continuously predict the battery's terminal voltage and a thermal model to continuously predict its temperature rise as charging progresses. The proposed optimization algorithm is based on a novel stepwise single-variable search technique that is very easy to implement and converges quickly. The results of our extensive simulation studies clearly indicate that the proposed charging strategy offers a fast, safe and easy-to-implement alternative to many of the existing computationally intensive optimal charging strategies.

Keywords: Li-ion batteries; fast charging; safe charging; optimal charge pattern

1. Introduction

Driven by the urge to comply with the clean air acts enacted by the governments around the world, the automotive manufacturers are moving toward electrification of their fleets, because powertrain electrification contributes significantly toward making cars clean and environmentally friendly [1], and lithium-ion batteries have emerged as the only plausible solution for driving powertrain electrification to the next level. There is also an ever-increasing demand for compact, low cost batteries for numerous applications ranging from portable and hand-held electronic devices to large electrical appliances. Over the last three decades, lithium-ion batteries have dominated both consumer electronics and electric vehicle markets, thanks to their falling price and continuous improvement of

their energy density [2]. However, they still suffer from two major drawbacks, namely, long charging times and limited capacity [3].

While material scientists are working on energy density improvement technologies [4], other researchers are focusing on the development of charging infrastructures and fast charging strategies, keeping into consideration capacity degradation due to battery aging and charging cycles [5]. It is well known that both charging methodology and operating temperature have significant effects on battery lifetime and battery performance [6], which give rise to the need for a robust battery management system (BMS) with an optimized charging strategy. To ensure a safe operation of Li-ion batteries, a BMS controls and monitors the state of each cell within the battery pack [7]. Besides measuring current, voltage, and temperature, a BMS also controls cooling, cell balancing, and power limits of the cells. This assures safe battery operation, as well as good performance and durability.

Before committing to the design phase of a BMS, it is essential to develop an accurate battery model. Such a model allows the prediction of long-term battery behavior as well as its performance. Various types of battery models proposed in the literature to date can be classified according to their accuracy and complexity. Some authors categorize them into physical, empirical and abstract (analogous) models [8]. While physical models offer a high level of accuracy by capturing the key features of the physical process, they have high computational time complexity, which can be problematic, especially if the model is required to run in real-time. Empirical models, on the other hand, provide a poor, simplistic representation of the system since they rely on experimental data instead of a mathematical representation of the system. Finally, abstract (analogous) models provide a trade-off between accuracy and simplicity. Although different types of analogous battery models can be constructed, electrical equivalent circuit (EEC) models are most popular and have found widespread use in BMS and other applications [8].

Furthermore, a BMS requires an optimum battery charging strategy to improve a battery's charge time without compromising its performance. According to Zhang et al. [9], battery charging strategies can be classified into four broad categories, namely, methods based on the improvement of the battery materials [10,11], polarization-based methods [12,13], methods based on improvement of the charging current [14–17], and methods based on the improvement of battery models [18–22]. All these methods are characterized by their relative advantages and disadvantages. For example, methods based on improvement of battery materials seem promising as researches are actively experimenting with different electrode and electrolyte materials to develop next-generation Li-ion batteries for improving specific energy and reducing the cost. However, an extensive amount of research and experimentation is needed to prove their safety and reliability for automotive and other applications. Similarly, the polarization-based methods are also of interest in the future because they provide a promising alternative, but they require further development and are more complicated compared to the methods based on improvements of charging current and battery models. The methods belonging to the last two categories are of special interest here, because the charging scheme presented in this paper is also based on similar principles.

Among the methods based on improvement of charging current, the older ones are of heuristic nature and lack mathematical rationality and basis. On the other hand, the newer methods, as exemplified by [14–17], are based on designing optimum current profiles that can lower charging time and prolong battery life. For instance, Guo et al. [14] proposed an EEC model based method of designing an optimum nonlinear current profile using genetic algorithm as an optimization tool. The proposed method is potentially useful for reducing charging time and prolonging cycle life. However,

one of the drawbacks of the proposed method is that it uses a highly nonlinear current profile and furthermore, it may not be suitable for time-critical applications because genetic algorithm has a relatively high computational time complexity. The other methods [15–17] can be regarded as variants of multistage constant current charging (MCC) charging strategies. For instance, Vo et al. [15] proposed a Taguchi method to search for an optimum MCC charging current profile. Compared with the traditional constant-current constant-voltage (CCCV) method, it can reduce the charging time, decrease the temperature variation, and improve energy efficiency. However, the computational time complexity of the proposed method is relatively high and therefore, it is not suitable for time-critical applications. Contrary to passive charging techniques, which utilize a fixed pre-set charging profile, an adaptive charging current would adapt with the variation of internal battery parameter changes during its cycle life. Such techniques can be broadly classified into two categories, namely, experiment-based methods and model-based methods, combined with some optimization technique [16,17]. Chen et al. [16] proposed a method searching for the optimal charging current pattern of a MCC current profile based on an EEC model and the grey wolf optimization technique. The proposed method is potentially useful for simultaneously reducing the charging loss and shortening the total charging time. In addition, this method can significantly reduce the temperature rise, and improve charging efficiency and battery life cycle. Jiang et al. [17] also proposed a hybrid charging strategy with adaptive current control, which is called CC-CC-CV strategy. It can also reduce the maximum temperature rise and energy losses.

Among the methods based on improvement of battery models [18–22], most of the methods proposed to date use either simplified electrochemical models [18–20] or EEC models [21,22] to develop fast charging strategies. Liu et al. [18] posed the problem of fast charging as a dynamic optimization problem that attempts to optimize the charging current trajectory of the battery to meet a desired target state of charge (SOC) subject to a side reaction constraint governing the rate of degradation via lithium-ion plating. They used a physics based model and employed Gauss pseudospectral method [GPM] to optimize the charging current trajectory. Xu et al. [19] proposed an optimal MCC charging strategy that not only minimizes the charging time but also attempts to minimize capacity fade due to solid electrolyte interphase (SEI) increase, decrease lithium plating, and reduce the temperature rise. The proposed method is based on an electrochemical battery model and optimization method employed is dynamic programming (DP). A similar approach was also proposed by Liu et al. [20], but they used genetic algorithm (GA) as the optimization tool. All the charging strategies mentioned above are interesting and useful for certain applications, but one of their major drawbacks stems from the fact that both the electrochemical models as well as the proposed optimization methods are computationally intensive and not suitable for time-critical applications that require fast search for optimal charge patterns. In contrast to the above methods, the EEC model based methods, as exemplified by [21,22], are much simpler to implement and therefore, potentially useful for time-critical applications. Both Hu et al. [21] and Zhang et al. [22] proposed EEC model based fast charging strategies that are based on solving a multi-objective optimization problem for simultaneously minimizing both charging time and charging losses. Their main difference lies in the choice of the optimization tool. Hu et al. [21] used large scale sequential quadratic programming (SQP) method, whereas Zhang et al. employed dynamic programming (DP). However, both SQP and DP are computationally intensive methods that are not suitable for time-critical applications, and there exists a need for developing faster optimization strategies.

From the above discussion, it is clear that EEC models are best suited for developing fast charging strategies that are going to be useful for time-critical applications. While minimizing charging time, however, attention must also be paid to battery safety issues, such as temperature rise and lithium plating. Thus, an EEC model needs to be augmented by ancillary models that account for some of the battery safety issues. Since Li-ion batteries are prone to thermal runaway, preventing excessive temperature rise during charging is deemed most critical. In fact, excessive temperature rise during charge/discharge operations can also cause capacity degradation, premature aging, and temperature related stresses. In view of this, we focus on developing a fast charging algorithm that not only minimizes the battery charging time, but also restricts its temperature rise. To achieve this dual objective, the charging algorithm proposed here utilizes an electro-thermal battery model that consists of an EEC battery model augmented with a thermal model. Such a coupled electro-thermal model can predict the battery's terminal voltage as well as the internal temperature of the battery [23,24]. Thus, such a model is useful in the quest for an optimal charge pattern, while restricting the battery's temperature within safe limits, thus ensuring operational safety and reducing stresses on the battery.

Having selected an electro-thermal battery model as the backbone of our fast charging strategy, the next important questions concern the selection of a charge current profile as well as selection of a thermal model. Both issues are discussed in details in Sections 2 and 3 below, but just to summarize the main principle, we would like to mention here that that a MCC charge pattern is chosen in this study because numerous researchers have found that compared to traditional CCCV charging method, which used to be popular in the past, MCC decreases total charging time and also reduces temperature rise [25,26]. Finally, as for the thermal model, an analytical-numerical (ANM) thermal model is adopted in this study because this model eliminates the need for measuring the core temperature of the battery, which is thought to be a hazardous task [27]. An ANM thermal model allows estimation of the core temperature instead of actually measuring it. Furthermore, just like an EEC model, an ANM thermal model offers a good trade-off between modeling accuracy and the ease of implementation.

In this paper, we present a multistage constant current (MCC) charge pattern optimization strategy that minimizes the total charge time of a Li-ion battery, while limiting its temperature rise within safe limits specified by the user. The main contributions here are two fold, namely, presentation of a fast optimum charging strategy that has very low computational time complexity compared to the existing charging strategies, and at the same time, restricting the temperature rise of the battery to a safe level specified by the user. The organization of this paper is as follows. Section 2 summarizes the basic principle of MCC charging method. Section 3 presents a brief overview of an electro-thermal model of a Li-ion battery. The problem of battery charge pattern optimization is discussed in Section 4, which also introduces the proposed fast charging algorithm. Section 5 presents the results of some simulation studies. Finally, some concluding remarks are provided in section 6.

2. Multistage constant current charging

Multistage Constant Current (MCC) charging method is the focus of this study because a number of researchers have shown its advantages, such as shorter charging time, lower temperature rise, and extended battery life [25]. Also, compared to the conventional constant current constant voltage (CCCV) charging method, MCC has been proven to be less stressful and safer [26]. The conventional CCCV charging method consists of two phases, a constant current (CC) phase where the battery is charged using a constant current until a cutoff voltage is reached, which is followed by a constant voltage (CV)

phase where the battery maintains that cutoff voltage until the charging current reaches the charging current reaches a near zero. Two key factors of CCCV are the charging current, I_{cc}, during CC phase and the cutoff voltage, V_{cv}, during CV phase. The cutoff voltage is typically chosen in accordance with the nominal cell voltage. For conventional Li-ion batteries, V_{cv} is chosen to be approximately 4.0 V. However, it should be noted that during CV mode, a constant stress is continuously applied to the battery while maintaining that cutoff voltage.

Contrary to CCCV, a multistage constant current (MCC) charging profile consists of N ($\geq$ 2) constant current charging stages with different current levels until the battery's cutoff voltage is reached. Typically, the charging current starts from a high initial value, which is reduced gradually in a stepwise fashion for each successive stage when a preset switching condition is met. In other words, the successive charging currents can be denoted by I_k, $1 \leq k \leq$ N and $I_k > I_{k+1}$. Since CV mode is not utilized during MCC charging, it presents a significant advantage over conventional CCCV. However, the performance of a MCC charging method is governed by many factors, such as the number of stages, N, charging currents, I_k, $1 \leq k \leq$ N, and the total charging time.

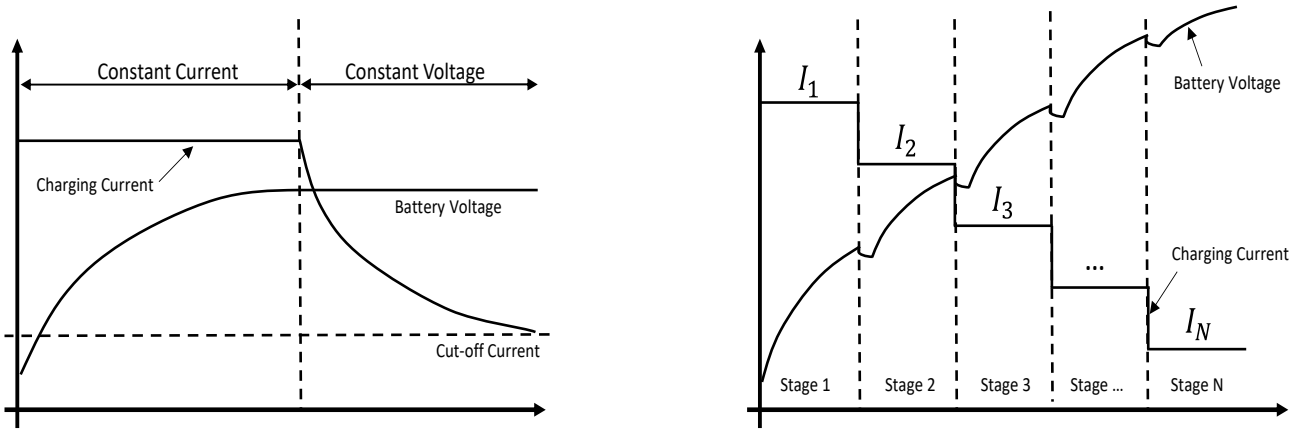

Figure 1. Current-voltage profiles of CCCV (on left) and MCC (on right) charging strategies.

3. Integrated Electro-Thermal Model of a Li-ion battery

The integrated electro-thermal model studied here is based on a coupled electrical equivalent circuit (EEC) model and a thermal battery model. The EEC model is used to predict the battery's terminal voltage during charge or discharge operations, while the thermal model estimates the temperature rise of the battery [23]. First, we discuss the EEC model and then summarize the thermal model.

3.1. Electrical Equivalent Circuit (EEC) Model

A simplified form of the voltage-current response circuit of a popular EEC model [28] is shown in Figure 2 below. This second order EEC battery model, characterized by five lumped parameters, has been widely used in literature to model the voltage-current relationship of a Li-ion battery during charge and discharge operations.

This circuit models the transient response of the battery when connected to an external load. The voltage-current response of a battery due to a step change in the load current exhibits both instantaneous characteristics as well as short-term and long-term transient characteristics. The instantaneous response is modeled by a series resistor, R_0, which basically represents the internal series resistance of the battery, whereas the short-term and long-term transients are modeled by a pair of parallel RC circuits, (R_1, C_1) and (R_2, C_2). Also, V_{ocv} represents the battery's open circuit voltage, which is a voltage-controlled voltage source dependent on the SOC.

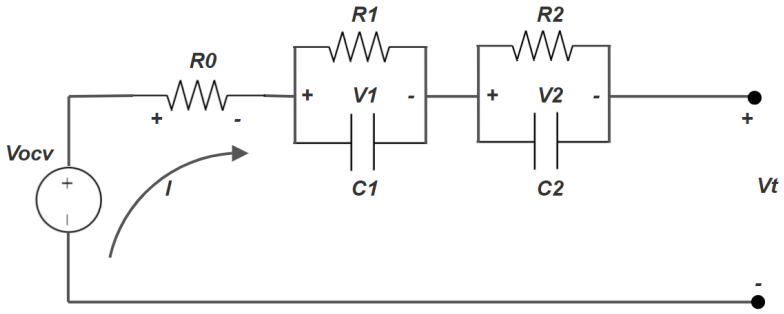

Figure 2. The voltage-current response circuit of an EEC battery model. V_{ocv} represents the battery's open circuit voltage, I denotes the current, and the short-term and long-term transients are modeled by a pair of parallel RC circuits.

The equations governing the circuit operation are given by:

$$\frac{d(soc)}{dt} = -\frac{1}{C_n} I \tag{1}$$

$$V_{ocv} = f(SOC) \tag{2}$$

$$V_T = V_{ocv} - V_1 - V_2 - IR_0 \tag{3}$$

where C_n denotes the battery capacity, I denotes the current, V_T is the terminal voltage and $f(SOC)$ is a known nonlinear function that models the relationship between open circuit voltage, V_{ocv}, and state of charge (SOC).

3.1.1. Remark 1

Although V_{OCV} is primarily a function of SOC, as pointed out by a number of researchers recently [30,31], it also depends (to a much lesser extent) on temperature. In fact, this temperature coefficient of voltage (TCV) is only of the order 0.1 mV/°C for Li-carbon anodes [31], but still for a high capacity battery, such as a 75 AH battery studied in [30], it may cause a V_{OCV} difference of about 25 mV for a temperature variation from 0 °C to 45 °C. Since this study focusses on a low capacity (2.3 AH) battery, and the temperature variation is typically restricted to below 10 °C, we ignore the temperature coefficient of voltage here and assume V_{OCV} is essentially a function of SOC. However, the results presented here can easily be extended to high capacity batteries and battery packs by adding a correction term due to TCV.

A state space representation of the circuit is given by the following equations:

$$\dot{V}_1 = -\frac{1}{R_1 C_1} V_1 + \frac{1}{C_1} I \tag{4}$$

$$\dot{V}_2 = -\frac{1}{R_2 C_2} V_2 + \frac{1}{C_2} I \tag{5}$$

where V_1 and V_2 denote the state variables, which represent the voltages across the capacitors, C_1 and C_2, respectively. It is also important to note that the parameters of the EEC model are time-varying and dependent on both temperature and SOC.

3.2. Thermal Model of a Li-ion battery

During charging of a Li-ion battery, heat is generated due to both Joule heating in the internal resistance of the battery and the entropic changes resulting from the associated chemical reactions. Thus, it is important to monitor the temperature of a battery during charging operations, because failure to do so may result in capacity degradation, premature aging, temperature related stresses, and other safety concerns. Since battery performance is highly dependent on temperature, it is important to limit the rise of temperature during battery operations. Battery thermal models have been found to be very useful for this purpose, because such models can be used to estimate the temperature rise of a battery during charging.

A wide variety of battery thermal models, suitable for different applications, have been proposed in the literature [32]. They differ from each other in their level of complexity, accuracy and computational cost. These models can be broadly divided into three categories, namely, lumped parameter models (LPM), finite element models (FEM), and analytical-numerical models (ANM). The LPM models are useful for fast simulation, but suffer from limited accuracy, whereas FEM models are highly accurate, but have a high (computational) time complexity, which precludes their usage in time-constrained applications. The ANM models, on the other hand, offer a reasonable trade-off between simulation accuracy and (computational) time complexity. In view of above, a simplified ANM thermal model has been adopted in this study.

A simplified ANM thermal model of a Li-ion battery is depicted in Figure 3 below [23,24]. A state space representation of this model is given by:

$$\dot{T}_c = \frac{Q}{C_c} + \frac{T_s - T_c}{R_c C_c} \tag{6}$$

$$\dot{T}_s = \frac{T_f - T_s}{R_u C_s} - \frac{T_s - T_c}{R_c C_s} \tag{7}$$

where C_c and C_s denote the lumped heat capacities of the core and casing, respectively. Also, R_c and R_u denote the heat conduction and convection resistances, respectively, and T_f, T_c and T_s denote the ambient, core, and surface temperatures, respectively. Moreover, Q is the heat generated during the chemical reaction of the battery, which includes the Joule heating due to over-potential and the heat generated due to entropy change. It can be expressed as:

$$Q = I(V_{OCV} - V_T) + IT_c \frac{dV_{ocv}}{dT_c} \tag{8}$$

However, according to [24], the effect of the entropic heat generation is often omitted for simplicity as its contribution to the overall heat generation is relatively small.

Also, the mean temperature, T_m, of the battery can be written as:

$$T_m = (T_c + T_s)/2 \tag{9}$$

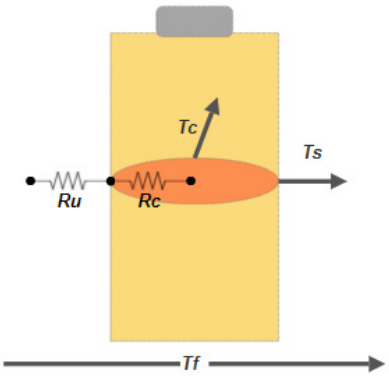

Figure 3. A simplified thermal model. R_c and R_u denote the heat conduction and convection resistances, respectively, and T_f, T_c and T_s denote the ambient, core, and surface temperatures, respectively.

3.3. Inter-coupling between the EEC and Thermal Models

An inter-coupling between the EEC and the thermal models is formed when the heat generated by the electrical model, Q, serves as an input to the thermal model. The core and surface temperatures are predicted by the thermal model, and its mean value, T_m, is used to update the values of the EEC model parameters [23]. The state vector, X, input, U, and output, Y, of the integrated electro-thermal model can be expressed as:

$$X = [V_1\ V_2\ T_c\ T_s]^T \tag{10a}$$

$$U = [I\ T_f] \tag{10b}$$

$$Y = V_T \tag{10c}$$

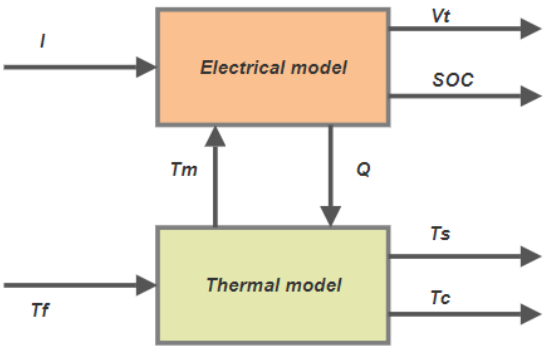

Figure 4. Coupled electro-thermal model. Model parameters are listed in Table 1.

Table 1. Electro-thermal Model parameters.

C_1, C_2	Capacity of the two RC circuits.
C_c, C_s	Core and surface lumped heat capacities.
C_n	Battery capacity.
I	Charging current.
Q	Heat generated by electrical circuit.
R_0	Internal resistance.
R_1, R_2	Resistance of the two RC circuits.
R_c, R_u	heat conduction and convection resistances.
T_c, T_s	Core and surface temperatures.
T_f	Ambient temperature.
T_m	Core and surface temperature mean value.
V_t	Terminal voltage.
V_1, V_2	Voltage across the two RC circuits

4. MCC charge pattern optimization strategy

A MCC charge pattern optimization method is presented in this section. Here the objective of optimization is to find a suitable charging pattern that minimizes the total charging time, while limiting the battery's temperature rise. The charge pattern optimization problem can be stated as follows.

4.1. Optimization problem 1

Find optimal values of $\{N, \Delta t_k \text{and } I_k, 1 \le k \le N\}$ that minimize the total charge time,t_N, subject to the constrains,

$$\sum_{k=1}^{N} \Delta T_k \le \Delta T_{max} \tag{11a}$$

$$\sum_{k=1}^{N} \Delta SOC_k = SOC_{Goal} \tag{11b}$$

where N denotes the number of stages, I_k is the charging current and t_k denotes the charge termination time for stage k, and $\Delta t_k = t_k - t_{k-1}$ represents the charging duration for stage k. Also, ΔT_k and ΔSOC_k denote the temperature-rise and SOC gain for stage k, ΔT_{max} is the maximum allowable temperature rise of the battery during charging, and SOC_{Goal} denotes the targeted SOC level.

The above optimization problem is difficult to solve unless some simplifying assumptions are introduced. In fact, most researchers assume that N is known a priori, and the allowable values of charge current levels, I_k, are assumed to be known fractions or multiples of the C-rate charge current, such as 0.5C, 1C, 1.5C, etc. [18,21,27]. Thus, a simplified version of the above problem can be expressed as:

4.1.1. Optimization problem 2

Find optimal values of $\{t_k, I_k, 1 \le k \le N\}$ that minimize the total charge time,t_N, subject to the constraints (11a–11b).

Many optimization techniques can be applied to find a solution to the above Optimization Problem 2, including a multi-objective optimization algorithm, such as minimax or goal programming,

or an evolutionary optimization method, such as genetic algorithm (GA) [33]. In fact, GA has been used by several researchers [18,21]. However, the solutions provided by GA should not be considered as optimal, but only quasi-optimal due to the following facts:

- The number of stages N is assumed to be known a priori;
- The presumed charging profile may not be optimal;
- A solution provided by GA is not guaranteed to be the global optimum. It can at best be a very good local optimal solution.

Furthermore, although GA can provide a good solution, it is rather slow to execute because it requires numerous random searches to find such a solution. Thus, GA and other evolutionary algorithms are not suitable for fast charging applications.

It is clear from the above discussion that the development of a fast charging algorithm calls for further simplification of Optimization Problem 2. To simplify the problem, we retain constraint (11b) as it is, but replace constraint (11a) by a new one related to temperature-rise in each stage, and define a simplified optimization problem as:

4.1.2. Optimization problem 3

For a given set of charge currents, $\{I_k, 1 \le k \le N\}$, find optimal values of $\{t_k, 1 \le k \le N\}$ that minimize the total charge time,t_N, subject to the constraints:

$$\Delta T_k \le \Delta T_{k,max} \tag{12a}$$

$$\sum_{k=1}^{N} \Delta SOC_k = SOC_{Goal} \tag{12b}$$

where $\Delta T_{k,max}$ represents the maximum (permitted) temperature rise for stage k, $1 \le k \le N$.

It may be pointed out that Optimization Problem 3 constitutes a new idea, which, at the cost of introducing some additional prior information, i.e., knowledge of I_k *and* $\Delta T_{k,max}$, $1 \le k \le N$, significantly reduces the time complexity of the optimization problem. The algorithm proposed below solves Optimization Problem 3.

4.2. Proposed fast charging algorithm

Notice that an optimal solution of Optimization Problem 3 would require a multivariable global minimization technique. However, the available global minimization algorithms are time-consuming and never guaranteed to yield the global optimal solution. In view of this, since the primary goal of this study is to develop a fast and safe charging strategy for time-constrained applications, we propose to use a quasi-optimal search strategy consisting of successive single variable searches to find the optimal values of $\{t_k, 1 \le k \le N\}$. Specifically, for the k^{th} charging stage, we find the optimal value of the charge termination time, t_k, by using a technique similar to interval-halving method [33], which is described below. Before describing the algorithm, first we introduce a few notations that are shown in Table 2 below.

Table 2. Notations used in the proposed fast charging algorithm.

Notation	Definition
N	No. of (MCC) stages.
I_k	Charging current for stage k.
t_0	Initial time.
t_k	Charge termination time for stage k.
t_{kL}, t_{kU}	Interval of uncertainty (IOU) for t_k, where t_{kL} and, t_{kU} denote the lower and upper bounds, respectively, of t_k.
t_{ol}	Tolerance (> 0), used to terminate search for t_k; for instance, $t_{ol} = 30/60$ sec.
t_M	Middle point of the interval of uncertainty.
t_N	Total charge time.
$SOC_{Initial}$	Initial SOC level.
SOC_{Goal}	Targeted SOC level.
SOC_{Accu}	SOC accumulated from the previous stages of MCC charge.
ΔSOC_k	Incremental SOC gain during stage k.
$\Delta T(I, dt)$	Battery's temperature rise due to charging at a constant current, I, for a duration, dt.
$\Delta T_{k,max}$	Maximum allowable temperature rise for stage k.

Fast charging algorithm

Step 1 (Initialization): Set $SOC_{Initial}$ and SOC_{Goal}. Choose N; I_k, $1 \le k \le N$; and $\Delta T_{k,max}$, $1 \le k \le N$. Initialize $SOC_{Accu} = SOC_{Initial}$; set $k = 1$.

Step 2: If $(SOC_{Accu} \ge SOC_{Goal}), stop; else$ start a search for an optimal t_k; let $t_{k\mathrm{L}} = 0$ and calculate $t_{k\mathrm{U}}$ as the time needed to completely charge the battery using charging current I_k:

$$t_{kU} = \frac{(SOC_{Goal} - SOC_{Accu}) * C_n}{I_k} \tag{13}$$

Step 3: Run thermal model to estimate the expected temperature-rise (if charged at current I_k for a duration, $t_{kU} - t_{k-1}$), *i.e.*, $\Delta T(I_k, t_{kU} - t_{k-1})$.

- If $\Delta T\ (I_k, t_{kU} - t_{k-1}) \le \Delta T_{k,max}$
  - set $t_k = t_{kU}$;
  - simulate electro-thermal battery model for $t \in (t_{k-1}, t_k)$;
  - $\Delta SOC_k = I_k(t_k - t_{k-1})$; $SOC_{Accu} = SOC_{Accu} + \Delta SOC_k$;
  - set $k = k + 1$;
  - go back to step 2 to proceed to the next stage.
- else $t_k \in (0, t_{kU})$, which is the interval of uncertainty (IOU) for t_k;
  - set $t_{kL} = 0$;
  - go to Step 4 to search for an optimal value of t_k

Step 4: (Interval-halving search for an optimal value of t_k)

4A. Find the middle point of the current IOU, $t_{kM} = \frac{(t_{kL} + t_{kU})}{2}$.

- If $(t_{kU} - t_{kL}) < tol$, stop further search for t_k;
  - set $t_k = t_{kM}$;
  - simulate electro-thermal battery model for $t \in (t_{k-1}, t_k)$;
  - $\Delta SOC_k = I_k(t_k - t_{k-1})$; $SOC_{Accu} = SOC_{Accu} + \Delta SOC_k$;
  - set $k = k + 1$;
  - go back to step 2 to proceed to the next stage.

- else proceed to step 4B below.

4B. Run thermal model to estimate the expected temperature rise (if charged at current I_k for a duration, $t_{kM} - t_{k-1}$), *i.e.* $\Delta T(I_k, t_{kM} - t_{k-1})$.

- If $\Delta T(I_k, t_{kM} - t_{k-1}) < \Delta T_{k,max}$, $t_k \in (t_{kM}, t_{kU})$, which is the new (reduced) IOU for t_k;
- set $t_{kL} = t_{kM}$, keep t_{kU} unchanged;
- go back to step 4A to continue interval-halving search.
- else if $\Delta T(I_k, t_{kM} - t_{k-1}) > \Delta T_{k,max}$, $t_k \in (t_{kL}, t_{kM})$, which is the new (reduced) IOU for t_k;
- set $t_{kU} = t_{kM}$, keep t_{kL} unchanged;
- go back to step 4A to continue interval-halving search.
- else if $\Delta T(I_k, t_{kM} - t_{k-1}) = \Delta T_{k,max}$,
- set $t_k = t_{kM}$;
- simulate electro-thermal battery model for $t \in (t_{k-1}, t_k)$;
- $\Delta SOC_k = I_k(t_k - t_{k-1})$; $SOC_{Accu} = SOC_{Accu} + \Delta SOC_k$;
- set $k = k + 1$; go back to step 2 to proceed to the next stage.

For better clarity, the above optimization procedure is also illustrated in the following flow chart.

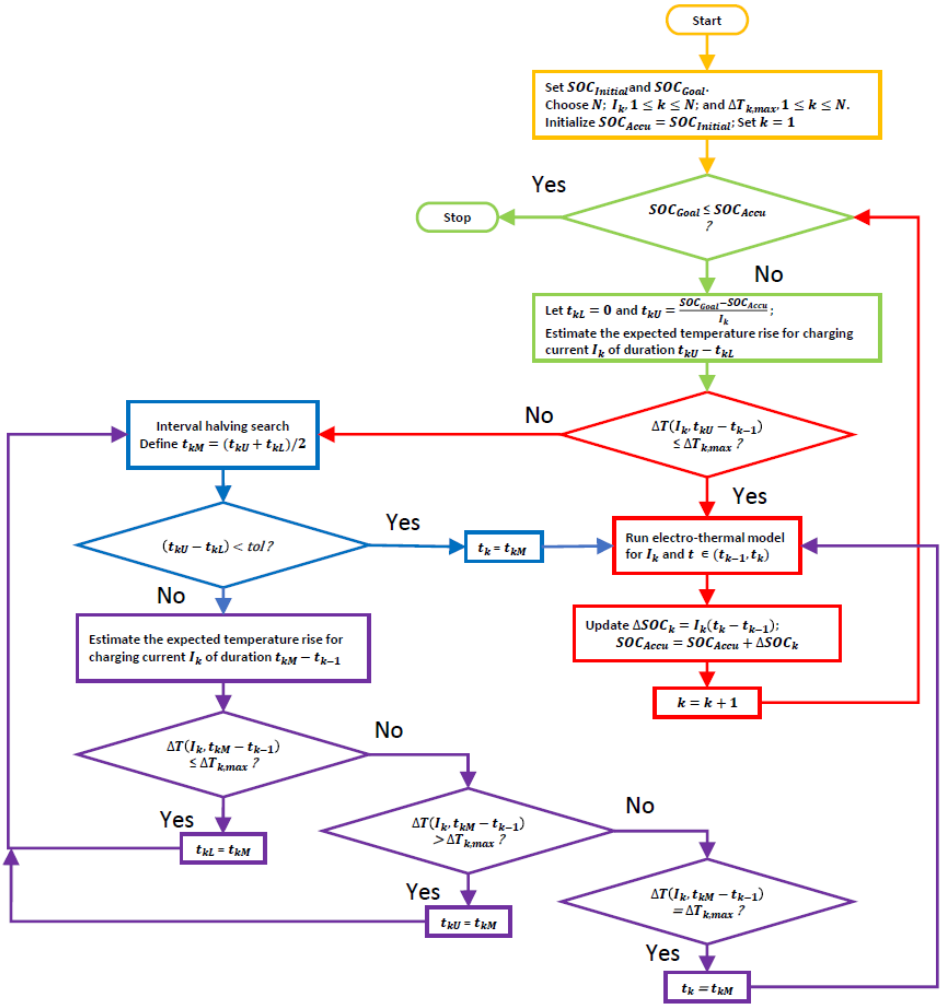

Figure 5. Flow chart of the proposed fast charging algorithm.

5. Results and discussion

The proposed quasi-optimal MCC charge pattern optimization strategy was simulated using an integrated electro-thermal battery model for a 2.3 AH A123-26650 Li-ion battery [23,34]. The electrical specifications and thermal model parameters of this battery that are used in this study, are summarized in Tables 3A and 3B below. This electro-thermal model has been experimentally verified to be reasonably accurate and used by a number of researchers for fast charging and other applications. Although the performance of the proposed optimization algorithm was evaluated by conducting an extensive set of simulation studies, the results of only four such studies are summarized here to illustrate its key properties.

Table 3A. Electrical specifications of A123-26650 battery [34].

Nominal Ratings		Charging	
Voltage	3.3 V	Recommended Charge Current	3 A
Capacity @ 25 ℃ Typ (Min)	2.6 Ah (2.5)	Max Continuous Charge Current	10 A
Energy @ 25 ℃	8.25 Wh	Max Pulse Charge Current (10s)	20 A
Specific Power @ 25 ℃, 2 sec pulse	> 4000 W/kg	Float Voltage	3.45 V
Impedance (1KHz AC) Typ	6 mΩ	Recommended charge Voltage & Cut-off Current	3.6 V, taper to 125 mA
		Temperature Range (reduce charging current to 250 mA when under 0 ℃)	0 ℃ to 55 ℃

Table 3B. Thermal Model Parameters of A123-26650 battery [23].

Parameters	Description	Values
C_c	Internal heat capacity	62.7 (J/K)
C_s	Surface hear capacity	4.5 (J/K)
R_c	Heat conduction resistance	1.94 (K/W)
R_u	Convection resistance	3.19 (K/W)

In all the case studies presented here, the ambient temperature is assumed to be 25 ℃, $SOC_{Initial}$ is set to 0%, and the SOC_{Goal} is set to 100%. Also, the number of MCC stages is chosen to be $N = 5$.

For the first sample case study, we choose maximum allowed overall temperature rise, $\Delta T_{max} = 9$ ℃. The values of the charging current levels and the maximum allowed temperature rise for the five MCC stages are chosen to be as follows:

$$\{I_k,\ 1 \le k \le 5\} = \{3.5\ 3\ 2.5\ 2\ 1.5\} \text{ (in C-rates)}, \tag{14a}$$

$$\{\Delta T_{k,max},\ 1 \le k \le 5\} = \{2\ 2\ 2\ 2\ 1\}\ (in\ ^oC). \tag{14b}$$

The simulation results, shown in blue color in Figures 6–9, indicate that the battery's core temperature rises to 33.9 ℃ and the total charge time is 1748 seconds.

For the second sample case study, we choose ΔT_{max}= 7 ℃. The values of the charging current levels and the maximum allowed temperature rise for the five MCC stages are chosen to be as follows:

$$\{I_k,\ 1 \le k \le 5\} = \{3\ 2.5\ 2\ 1.5\ 1.2\}\ \text{(in C-rates)}, \tag{15a}$$

$$\{\Delta T_{k,max},\ 1 \le k \le 5\} = \{1\ 1\ 1\ 2\ 2\}\ (in\ ^oC). \tag{15b}$$

The simulation results, shown in red color in Figures 6–9, indicate that the battery's core temperature rises to 31.2 ℃ and the total charge time is 2340 seconds.

For the third sample case study, we choose ΔT_{max} = 5 ℃. The values of the charging current levels and the maximum allowed temperature rise for the five MCC stages are chosen to be as follows:

$$\{I_k,\ 1 \le k \le 5\} = \{2.5\ 2\ 1.7\ 1.5\ 1.2\}\ \text{(in C-rates)}, \tag{16a}$$

$$\{\Delta T_{k,max},\ 1 \le k \le 5\} = \{1\ 1\ 0.5\ 0.5\ 1\}\ (in\ ^oC). \tag{16b}$$

The simulation results, shown in gray color in Figures 6–9, indicate that the battery's core temperature rises to 29.8 ℃ and the total charge time is 2780 seconds.

A comparison of the above three case studies illustrates the trade-off between ΔT_{max} and total charge time t_N, namely, a gradual decrease of ΔT_{max} results in a concomitant increase of total charge time. This is in accordance with our expectation, because a lower ΔT_{max} would necessitate lower heat dissipation in the battery, or equivalently, lower charging currents, which would increase the total charge time.

In the last sample case study, we demonstrate that a significantly faster charging can indeed be achieved at the cost of a higher overall temperature rise. For this case study, we chose ΔT_{max}= 12 ℃. The values of the charging current levels and the maximum allowed temperature rise for the five MCC stages are chosen to be as follows:

$$\{I_k,\ 1 \le k \le 5\} = \{4\ 3.5\ 3\ 2.5\ 2\}\ \text{(in C-rates)}, \tag{17a}$$

$$\{\Delta T_{k,max},\ 1 \le k \le 5\} = \{2\ 2\ 2\ 2\ 1\}\ (in\ ^oC). \tag{17b}$$

The simulation results, shown in yellow color in Figures 6–9, indicate that the total charge time is now reduced to 1450 seconds, at the cost of an overall core temperature rise to 36.5 ℃.

Finally, to allow a quick comparison of the achievable trade-offs between ΔT_{max} and total charge time, t_N, a summary of the above four case studies is provided in Table 4 below.

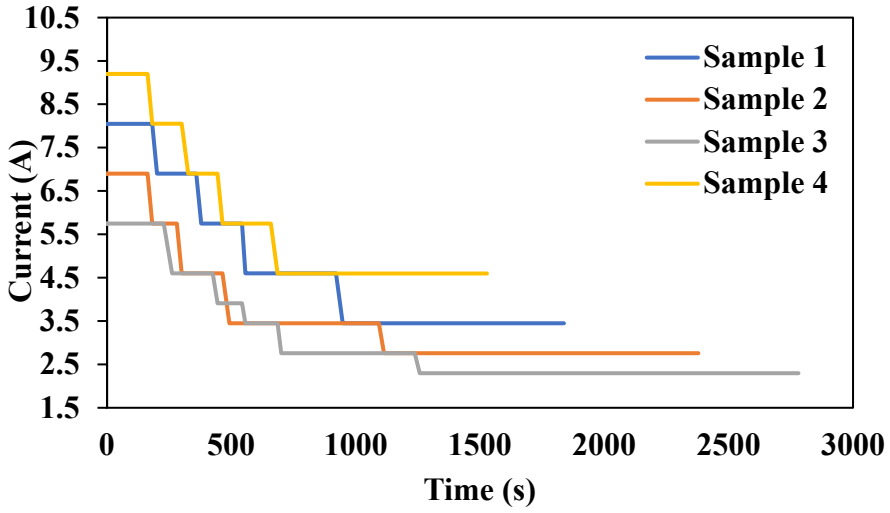

Figure 6. Optimum MCC charge profiles found for four sample case studies. For Sample case 1 (Blue), $\Delta T_{max} = 9$ ℃. The charging current levels and the maximum allowed temperature rise for the five MCC stages are given by Eq 14a and 14b. For Sample case 2 (Red), $\Delta T_{max} = 7$ ℃. The charging current levels and the maximum allowed temperature rise for the five MCC stages are given by Eq 15a and 15b. For Sample case 3 (Grey), $\Delta T_{max} = 5$ ℃. The charging current levels and the maximum allowed temperature rise for the five MCC stages are given by Eq 16a and 16b. For Sample case 4 (Yellow), $\Delta T_{max} = 12$ ℃. The charging current levels and the maximum allowed temperature rise for the five MCC stages are given by Eq 17a and 17b.

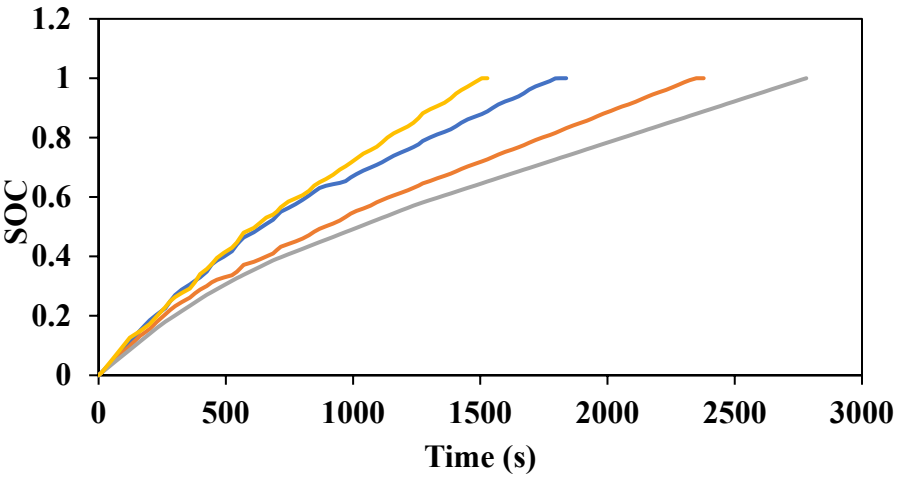

Figure 7. Evolution of battery's SOC for four sample case studies. See caption of Figure (6) for a detailed description of the parameters chosen for these case studies.

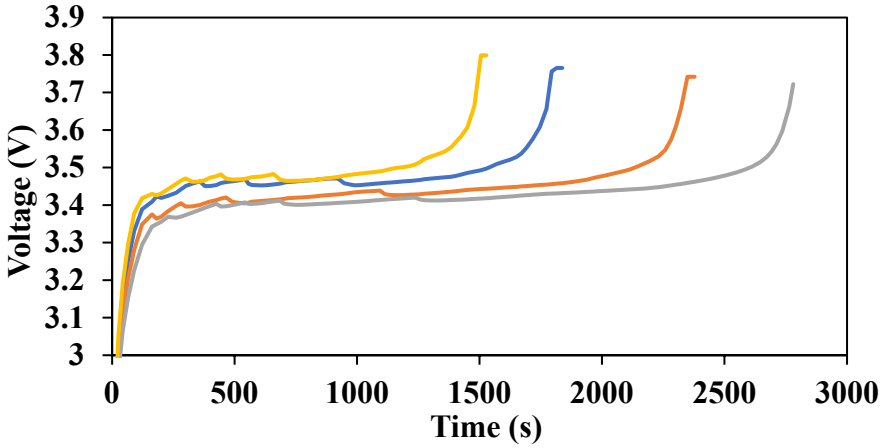

Figure 8. Evolution of battery's Terminal Voltage for four sample case studies. See caption of Figure (6) for a detailed description of the parameters chosen for these case studies.

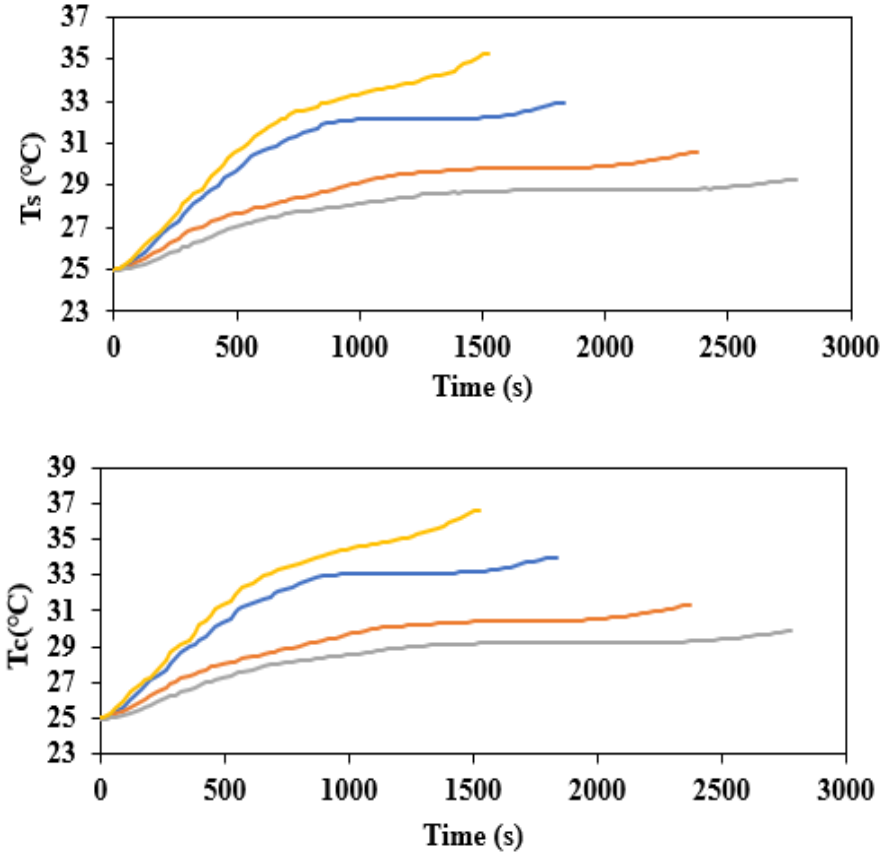

Figure 9. Evolution of battery's core temperature (T_c) and surface temperature (T_s) for the four case studies. See caption of Figure (6) for a detailed description of the parameters chosen for these case studies.

Table 4. A summary of four sample case studies.

Charge Current Levels for the five MCC Stages (in C-rates)					Total Charge Time (s)	T_c(℃)	T_s(℃)	ΔT_{max}(℃)
I1	I2	I3	I4	I5				
3.5	3	2.5	2	1.5	1748	33.9	32.8	9
3	2.5	2	1.5	1.2	2340	31.2	30.5	7
2.5	2	1.7	1.5	1.2	2780	29.8	29.2	5
4	3.5	3	2.5	2	1450	36.5	35.2	12

6. Conclusions

This paper presents an electro-thermal model based quasi-optimal multistage constant current charging algorithm for Li-ion batteries. The search for an optimal charge pattern is carried out on a stage by stage basis by restricting the temperature rise at each stage within safe limits. The algorithm consists of a sequence of successive one-dimensional searches for each stage, which is very easy to implement and suitable for fast charging applications. The proposed charging algorithm was simulated based on an integrated electro-thermal model of a 2.3 AH A123-26650 Li-ion battery, and the simulation results indicate that the algorithm performs as expected and can serve as an useful, easy-to-implement alternative to existing computationally intensive optimal charging strategies proposed by other researchers. However, as mentioned earlier, the proposed method only provides a quasi-optimal solution, because it is based on a sequential single variable search technique instead of a multivariable search method. Our on-going research is geared toward addressing the above shortfall.

Funding

This research did not receive any specific grant from funding agencies in the public, commercial, or not-for-profit sectors.

Conflict of interest

The authors declare that there is no conflict of interest in this paper.

References

1. Burch I, Gilchrist J (2018) Survey of Global Activity to Phase Out Internal Combustion Engine Vehicles. *Center of Climate Protection: Santa Rosa, CA, USA*.
2. Deng D (2015) Li-ion batteries: basics, progress, and challenges. *Energy Sci Eng* 3: 385–418.
3. Liu K, Zou C, Li K (2018) Charging pattern optimization for lithium-ion batteries with an electrothermal-aging model. *IEEE Trans Ind Inf* 14: 5463–5474.
4. Zhao J, Liao L, Shi F, et al. (2017) Surface fluorination of reactive battery anode materials for enhanced stability. *J Am Chem Soc* 139: 11550−11558.
5. Dong J, Liu C, Lin Z (2014) Charging infrastructure planning for promoting battery electric vehicles: An activity-based approach using multiday travel data. *Transp Res Part C Emerg Technol* 38: 44–55.

6. Leng F, Tan C, Pecht M (2015) Effect of temperature on the aging rate of Li Ion battery operating above room temperature. *Sci Rep* 5: 12967.
7. Cheng K, Divakar B, Wu H, et al. (2011) Battery-Management System (BMS) and SOC development for electrical vehicles. *IEEE Trans Veh Technol* 60: 76–88.
8. Saidani F, Hutter F, Scurtu R, et al. (2017) Lithium-ion battery models: A comparative study and a model-based powerline communication. *Adv Radio Sci* 15: 83–91.
9. Zhang C, Jiang J, Gao Y, et al. (2017) Charging optimization in lithium-ion batteries based on temperature rise and charge time. *Appl Energy* 194: 569–577.
10. Yanga X, Zhang G, Ge S, et al. (2018) Fast charging of lithium-ion batteries at all temperatures. *Proc National Acad Sci* 115: 7266–7271.
11. Kim K, Lee Y, Kang K, et al. (2012) A simple method for solving the voltage overshoots of LiFePO4-based lithium-ion batteries with different capacity classes. *RSC Adv* 2: 3844–3849.
12. Jiang J, Zhang C, Wen J, et al. (2013) An optimal charging method for Li-ion batteries using a fuzzy-control approach based on polarization properties. *IEEE Trans Veh Technol* 62: 3000–3009.
13. Choi S, Lim H (2002) Factors that affect cycle-life and possible degradation mechanisms of a Li-ion cell based on $LiCoO_2$. *J Power Sources* 111: 130–136.
14. Guo Z, Liaw B, Qiu X, et al. (2015) Optimal charging method for lithium-ion batteries using a universal voltage protocol accommodating aging. *J Power Sources* 274: 957–964.
15. Vo T, Chen X, Shen W, et al. (2015) New charging strategy for lithium-ion batteries based on the integration of Taguchi method and state of charge estimation. *J Power Sources* 273: 413–422.
16. Chen G, Liu Y, Wang S, et al. (2021) Searching for the optimal current pattern based on grey wolf optimizer and equivalent circuit model of Li-ion batteries. *J Energy Storage* 33: 101933.
17. Jiang L, Li Y, Ma J, et al. (2020) Hybrid charging strategy with adaptive current control of Lithium-ion battery for electric vehicles. *Renewable Energy* 160: 1385–1395.
18. Liu J, Li G, Fathy K (2016) A computationally efficient approach for optimizing lithium-ion battery charging. *J Dyn Syst Meas Control* 138: 1009-1–1009-8.
19. Xu M, Wang R, Zhao P, et al. (2019) Fast charging optimization for lithium-ion batteries based on dynamic programming algorithm and electrochemical-thermal-capacity fade coupled model. *J Power Sources* 438: 227015.
20. Liu C, Gao Y, Liu L (2021) Toward safe and rapid battery charging: Design optimal fast charging strategies thorough a physics-based model considering lithium plating. *Int J Energy Res* 45: 2303–2320.
21. Hu X, Li S, Peng H, et al. (2013) Charging time and loss optimization for LiNMC and LiFePO4 batteries based on equivalent circuit models. *J Power Sources* 239: 449–457.
22. Zhang S, Zhang C, Xiong R, et al. (2014) Study on the optimal charging strategy for lithium-ion batteries used in electric vehicles. *Energies* 7: 6783–6797.
23. Lin X, Perez H, Mohan S, et al. (2014) A lumped-parameter electro-thermal model for cylindrical batteries. *J Power Sources* 257: 1–11.
24. Forgez C, Do D, Friedrich G, et al. (2010) Thermal modeling of a cylindrical $LiFePO_4$/graphite lithium-ion battery. *J Power Sources* 195: 2961–2968.
25. Luo Y, Liu Y, Wang S (2009) Search for an optimal multistage charging pattern for lithium-ion batteries using the Taguchi approach. *Tencon 2009 IEEE Region 10 Conf*: 1–5.
26. Lu B, Zhao Y, Song Y, et al. (2018) Stress limited fast charging methods with time varying current in lithium-ion batteries. *Electrochim Acta* 288: 144–152.

27. Novais S, Nascimento M, Grande L, et al. (2016) Internal and external temperature monitoring of a Li-ion battery with fiber Bragg grating sensors. *Sensors* 16: 1394.
28. Chen M, Mora G (2006) Accurate electrical battery model capable of predicting runtime and I-V performance. *IEEE Trans Energy Convers* 21: 504–511.
29. Zhang X, Kong X, Li G, et al. (2014) Thermodynamic assessment of active cooling/heating methods for lithium-ion batteries of electric vehicles in extreme conditions. *Energy*: 64: 1092–1101.
30. Zhang R, Xia B, Li B, et al. (2018) A study on the open circuit voltage and state of charge characterization of high capacity lithium-ion battery under different temperature. *Energies* 11: 2408.
31. Swiderska-Mocek A, Rudnicka E, Lewandowski A (2019) Temperature coefficients of Li-ion battery single electrode potentials and related entropy changes—revisited. *Phys Chem Chem Phys* 21: 2115–2120.
32. Shabani B, Biju M (2015) Theoretical modelling methods for thermal management of batteries. *Energies* 8: 10153–10177.
33. Rao S (2009) *Engineering Optimization: Theory and Practice*. 4th Ed, John Wiley and Sons, Hoboken New Jersey.
34. LithiumWerks 26650 Lithium Ion Power Cell Datasheet. Available from: https://a123batteries.com/product_images/uploaded_images/26650.pdf.

AIMS Press